JTTEE5 8:433-439

Microstructure and Properties of Tungsten Carbide Coatings Sprayed with Various High-Velocity Oxygen Fuel Spray Systems

R. Schwetzke and H. Kreye

(Submitted 9 July 1998; in revised form 10 February 1999)

This article reports on a series of experiments with various high-velocity oxygen fuel spray systems (Jet Kote, Top Gun, Diamond Jet (DJ) Standard, DJ 2600 and 2700, JP-5000, Top Gun-K) using different WC-Co and WC-Co-Cr powders. The microstructure and phase composition of powders and coatings were analyzed by optical and scanning electron microscopy and x-ray diffraction. Carbon and oxygen content of the coatings were determined to study the decarburization and oxidation of the material during the spray process. Coatings were also characterized by their hardness, bond strength, abrasive wear, and corrosion resistance. The results demonstrate that the powders exhibit various degrees of phase transformation during the spray process depending on type of powder, spray system, and spray parameters. Within a relatively wide range, the extent of phase transformation has only little effect on coating properties. Therefore, coatings of high hardness and wear resistance can be produced with all HVOF spray systems when the proper spray powder and process parameters are chosen.

Keywords decarburization, high-velocity oxygen fuel, HVOF, phase transformation, tungsten carbide coatings, WC-Co, WC-Co-Cr

1. Introduction

Tungsten carbide based powders are widely used in high-velocity oxygen fuel (HVOF) spraying to produce dense coatings of high hardness and excellent wear resistance. In applications where abrasive wear or erosion resistance is of primary importance, WC-Co powders with 12 or 17 wt% Co are used, whereas WC-Co-Cr powders are preferred when higher demands on corrosion resistance are made. However, the microstructure and the properties of the coatings not only depend on the composition of the powder, they are also considerably affected by phase transformations occurring during the spray process. The WC-Co and WC-Co-Cr coatings can contain various amounts of phases such as W_2C, tungsten, and mixed carbides (η-phases M_6C and $M_{12}C$), resulting from an oxidation of the spray material in the flame and from thermally activated reactions between WC and the cobalt or cobalt-chromium matrix, respectively (Ref 1-6). Furthermore, rapid solidification of the supersaturated cobalt (tungsten, carbon) matrix can cause the formation of an amorphous or nanocrystalline phase (Ref 7-9). Phase transformations and the resulting coating characteristics are affected by the type and composition of the powder as well as by the spray system and the fuel used (Ref 10-15).

This article describes the phase transformations in more detail. Different spray systems, fuels, and powders were used to explore the extent that phase transformations are affected by the various process parameters and how they can be controlled to optimize coating properties.

This paper originally appeared in *Thermal Spray: Meeting the Challenges of the 21st Century; Proceedings of the 15th International Thermal Spray Conference,* C. Coddet, Ed., ASM International, Materials Park, OH, 1998. This proceedings paper has been extensively reviewed according to the editorial policy of the *Journal of Thermal Spray Technology.*

R. Schwetzke and **H. Kreye,** University of the Federal Armed Forces, Hamburg, Germany. Contact e-mail: werkstoff.technik@unibw-hamburg.de.

2. Experiments

2.1 Spray Experiments

In a first series of experiments all coatings were produced with the same powder, an agglomerated and sintered WC-Co 83-17 with a particle size range of –45 + 10 μm. The powder was sprayed with the HVOF systems Jet Kote (Stellite Coatings, Goshen, IN), Top Gun (UTP Schweißmaterial, Bad Krozingen, Germany), Diamond Jet (DJ) Standard, DJ 2600, DJ 2700 (Sulzer Metco, Westbury, NY), JP-5000 (Tafa, Concord, NH) and Top Gun-K (GTV, Luckenbach, Germany). Table 1 gives the various fuels and the process parameters used in the experiments.

A second series of experiments studied the effect of powder composition and powder type on coating characteristics. Seven different commercially available powders of WC-Co and WC-Co-Cr were selected for these experiments, as summarized in Table 2. The powders were sprayed with a DJ 2700 system using propane as fuel gas and the process parameters given in Table 1.

All coatings were sprayed on degreased and grit blasted mild steel substrates. The thickness of the coatings was between 180 and 300 μm. In addition, powder particles were sprayed into water and collected to study their melting behavior by scanning electron microscopy (SEM).

2.2 Investigation of Powders and Coatings

The morphology and the structure of the spray powders were characterized by scanning electron microscopy. The microstructure of the coatings was investigated on cross sections by optical and scanning electron microscopy including energy dispersive x-ray analysis (EDXA). The phase composition of the powders and the coatings was analyzed by x-ray diffraction using Co-Kα radiation. Carbon and oxygen content of powders and coatings were determined by the method of combustion and infrared detection.

The microhardness of the coatings was determined on polished cross sections using a Vickers diamond pyramid indentor with a load of 300 g. A minimum of ten readings was taken for each specimen. Microstructural investigations, phase analysis, and hardness tests were also performed on coatings annealed in an evacuated quartz tube for 1 h at 400, 500, 600, 700, and 800 °C to study changes of hardness and microstructure caused by these heat treatments.

The tensile bond strength of the coatings was measured by an adhesion test according to the European Standard EN 582 (Ref 16) using coated samples with a diameter of 25 mm. Abrasive wear tests were performed by a grinding wheel test according to the Japanese Standard JIS H 8615 (Ref 17). In this test a stationary wheel wrapped with an adhesive strip of 320 grit SiC abrasive paper was pressed against the coating with a load of 30 N and moved repeatedly back and forth over a distance of 30 mm. After each double stroke (DS) the wheel was set to rotate by 0.9° so that a new part of grit paper was used for the next double stroke. After one revolution of the wheel (400 DS) the grit paper was replaced. Wear was determined by the mass loss of the specimen after 1200 DS.

Corrosion tests were carried out using the Kesternich test (atmosphere of SO_2) and the salt spray test (NaCl solution) in accordance to the German Standards DIN 50018 and 50021 (Ref 18, 19), respectively. After the tests the mass loss of the corroded specimens was determined, and metallographic investigations were conducted to study the corrosion attack and the corrosion mechanism.

3. Results and Discussion

3.1 Structure and Chemistry of the Powders

The different spray powders showed morphologies and microstructures typical for the various manufacturing methods. The agglomerated and sintered powders were nearly spherical with a certain degree of porosity, whereas all the other powders

Table 1 Spray parameters and properties of WC-Co 83-17 coatings sprayed with various high-velocity oxygen fuel systems and fuels

High velocity oxygen-fuel system	Fuel	Fuel flow, m^3/h	Oxygen flow, m^3/h	Oxygen/ fuel ratio	Powder feed rate, g/min	Carbon content, wt%	Carbon loss, %	Hardness, 0.3 HV	Abrasive wear, mg/1200 DS
Jet Kote	Hydrogen	25.5	12.8	0.5	30-40	3.8	27	1080	4.0
	Propane	3.0	18.0	6.0	30-40	2.8	46	1200	3.3
	Ethylene	4.8	28.4	5.9	30-40	3.1	40	1240	2.9
Top Gun	Hydrogen	26.0	13.0	0.5	30-40	1.7	67	1080	8.4
	Propane	3.0	15.0	5.0	30-40	2.2	58	1240	3.8
	Ethylene	4.7	14.1	3.0	30-40	2.1	60	1110	5.5
DJ Standard	Propane	4.4	15.8	4.6	40-50	3.4	35	980	4.5
DJ 2600	Hydrogen	38.2	12.8	0.45(a)	60-70	3.2	38	1340	3.0
DJ 2700	Propane	4.1	14.5	4.6(a)	60-70	3.5	33	1390	2.9
	Ethylene	6.8	15.0	2.9(a)	60-70	3.1	40	1400	3.5
JP-5000	Kerosene	20.8 l/h	53.6	4.3(b)	80	3.3	37	1490	3.6
Top Gun-K	Kerosene	18.0 l/h	55.0	5.1(b)	80	3.7	29	1330	3.1

Spray powder: WC-Co 83-17, agglomerated sintered, –45 + 10 μm, carbon content 5.2 wt%. DS, double stroke. (a) Including the oxygen fraction of the compressed air. (b) Standardized mass ratio oxygen/kerosene.

Table 2 Properties of powders and coatings sprayed with a Diamond Jet 2700 system and propane as fuel gas

Powder	Powder type	Particle size, μm	Deposition efficiency, %	Carbon content, wt%		Carbon loss, %	Hardness, 0.3 HV	Abrasive wear, mg/1200 DS
				Powder	Coating			
WC-Co 83-17	Agglomerated sintered	–45 + 10	52	5.2	3.5	33	1390	2.9
WC-Co 88-12	Agglomerated sintered	–45 + 10	57	5.4	4.1	24	1310	2.8
WC-Co 88-12	Sintered	–45 + 5.6	49	5.2	4.2	19	1100	3.2
WC-Co 88-12	Fused	–45 + 10	52	4.2	3.9	7	1150	3.5
WC-Co-Cr 86-10-4	Sintered crushed	–45 + 11	56	5.2	4.7	10	1260	3.4
WC-Co-Cr 86-10-4	Sintered	–45 + 15	38	3.8	3.6	5	1290	5.5
WC-Co-Cr 86-6-8	Sintered	–45 + 15	55	5.6	4.7	16	1330	3.3

DS, double stroke

showed angular, blocky particle shapes and were fairly dense. All powders contained carbides of an average grain size from 2 to 8 μm in a relatively uniform distribution. Figure 1 shows scanning electron micrographs of different powders.

In the agglomerated and sintered powders and the sintered WC-Co powder only the WC and cobalt phases were detected by x-ray analysis. The other powders, in addition, contained various amounts of Co_3W_3C and W_2C, as listed in Table 3. The carbon content of the various powders ranged from 3.8 to 5.6 wt% (Table 2). Higher carbon contents, close to the stoichiometric composition, were found in the agglomerated and sintered powders and in the sintered powder of WC-Co 88-12, whereas lower carbon contents were found in the fused powder of WC-Co 88-12 and in the sintered powder of WC-Co-Cr 86-10-4. Lower carbon contents correlate with higher amounts of Co_3W_3C. The oxygen content of most powders was less than 0.08 wt%, except for the sintered (0.12 wt%) and the fused powder of WC-Co 88-12 (0.24 wt%).

Table 3 Phases present in the spray powders

Powder	Type	Identified phases
WC-Co 83-17	Agglomerated sintered	WC,Co
WC-Co 88-12	Agglomerated sintered	WC, Co
WC-Co 88-12	Sintered	WC, Co
WC-Co 88-12	Fused	WC, Co_3W_3C, W_2C
WC-Co-Cr 86-10-4	Sintered crushed	WC, Co_3W_3C, Co
WC-Co-Cr 86-10-4	Sintered	WC, Co_3W_3C, Co
WC-Co-Cr 86-6-8	Sintered	WC, Co_3W_3C, Co

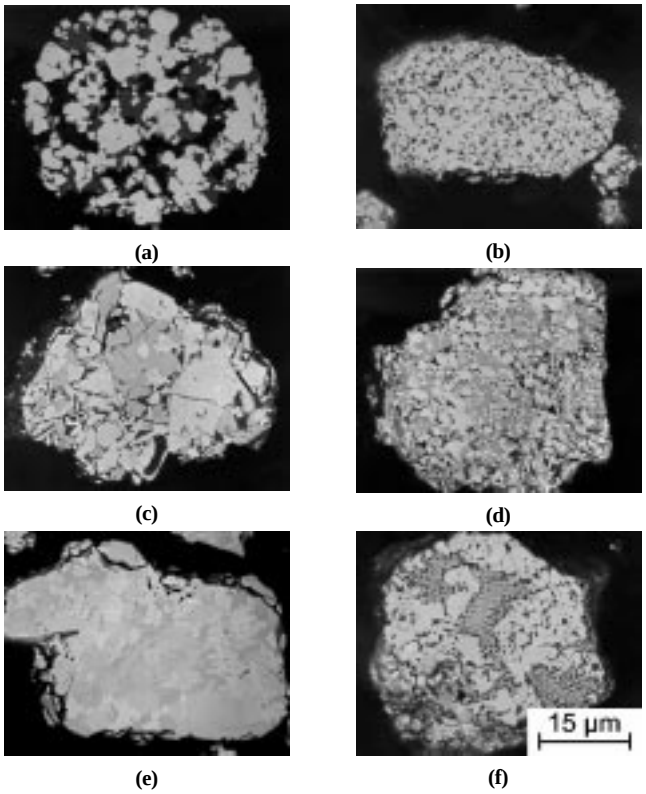

Fig. 1 Microstructure of the spray powders. (a) WC-Co 83-17 agglomerated and sintered. (b) WC-Co 88-12 sintered. (c) WC-Co 88-12 fused. (d) WC-Co-Cr 86-10-4 sintered and crushed. (e) WC-Co-Cr 86-10-4 sintered. (f) WC-Co-Cr 86-6-8 sintered

3.2 Microstructure and Chemistry of the Coatings

Coatings produced with the different spray systems, fuels, and powders, listed in Tables 1 and 2, showed a relatively dense structure and a homogeneous distribution of carbides, as demonstrated by optical micrographs in Fig. 2. Porosity was between 0.5 and 2.0% and seemed to be slightly higher for coatings produced with powders of a dense structure. However, there was a remarkable difference of these coatings with regard to the carbon content and the phases present in the coating, due to different degrees of oxidation and thermally activated transformation of WC and cobalt in the spray process.

Carbon loss for coatings sprayed with the agglomerated and sintered powder of WC-Co 83-17 varied from 25 to 70%. The extent of the carbon loss depended particularly on the spray system used, whereas the degree of decarburization increased with higher heating of the particles. In the experiments of the first series, carbon loss and the amount of amorphous and η-phases

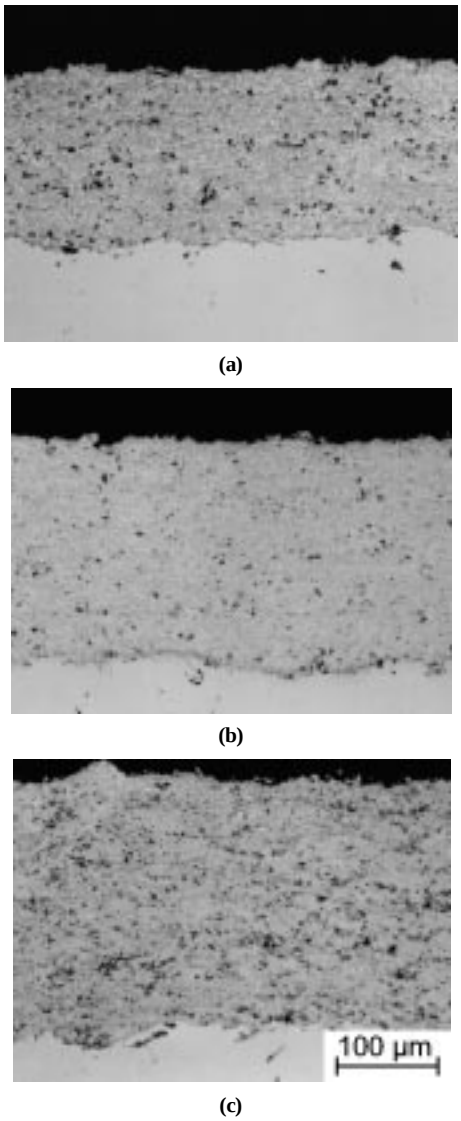

Fig. 2 Microstructure of WC coatings. (a) WC-Co 83-17, Jet Kote/propane. (b) WC-Co 83-17, DJ 2700/propane. (c) WC-Co-Cr 86-6-8, DJ 2700/propane

formed were highest when coatings were sprayed with the Top Gun system and low when using the DJ systems, the JP-5000, or the Top Gun-K system, as shown in Table 1. In the gas operated Top Gun system, particles are axially and centrically injected into the hottest zone of the flame, whereas in the kerosene operated systems JP-5000 and Top Gun-K the powder enters the flame behind the combustion chamber at a several hundred degree lower flame temperature. Also a higher flame temperature of the applied fuel increases the carbon loss during the spray process, whereas the oxygen/fuel ratio seemed to have only a small effect on the decarburization, possibly due to the lower flame temperature at high oxygen surplus.

Decarburization also depended on the type and composition of the powder, as shown in Table 2. Powders containing less carbon and already a considerable amount of η-phase exhibited lower carbon loss in the spray process. In addition the higher density of sintered or fused powders lowered the decarburization due to less heating of the particles.

The oxygen content of all coatings was between 0.08 and 0.80 wt%. The higher oxygen contents (0.30 to 0.80 wt%) were found in the coatings of WC-Co-Cr due to the preferred oxidation of chromium in the matrix. The oxygen content of all WC-Co coatings was less than 0.20 wt%.

3.3 Phase Transformations

The formation of W_2C and tungsten occurs by decarburization of WC. In the coatings, the WC grains are surrounded by a seam of W_2C, as demonstrated in Fig. 3, and a thin layer of tung-

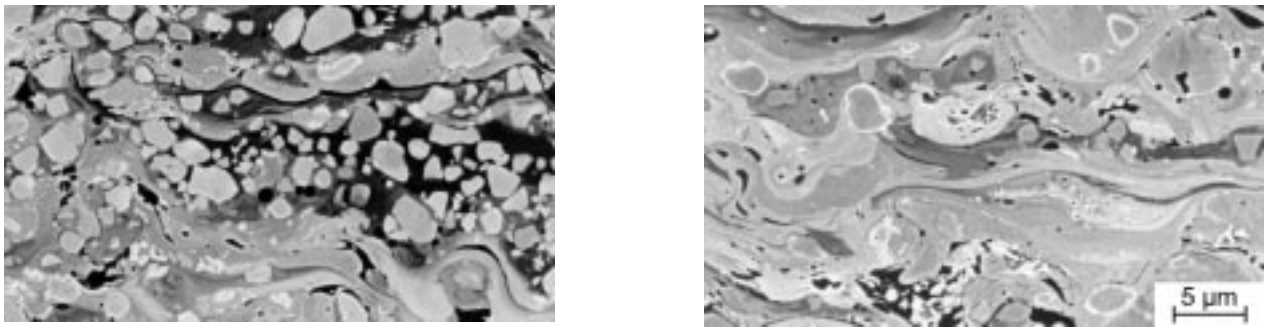

Fig. 3 Scanning electron micrographs of WC-Co 83-17 coatings. (a) Jet Kote/propane. (b)Top Gun/ethylene

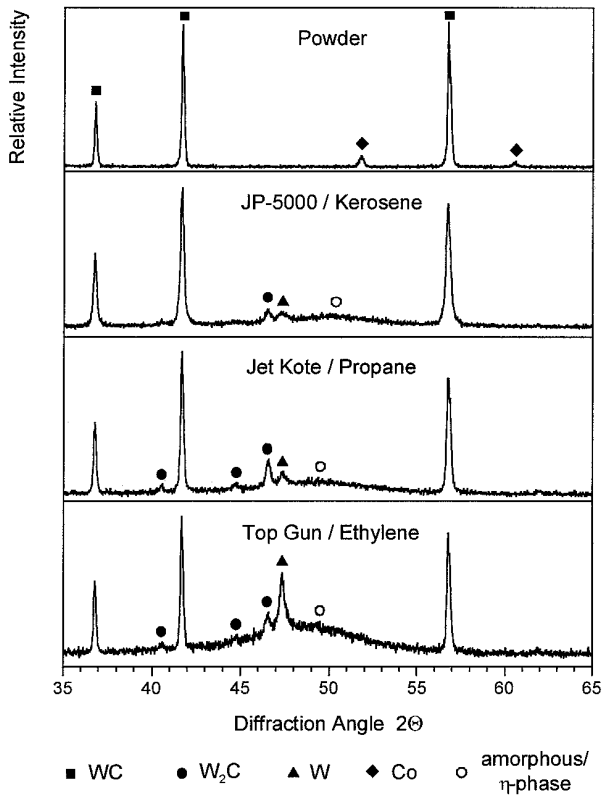

Fig. 4 X-ray diffractograms of powder and coatings of WC-Co 83-17 with different degrees of phase transformations

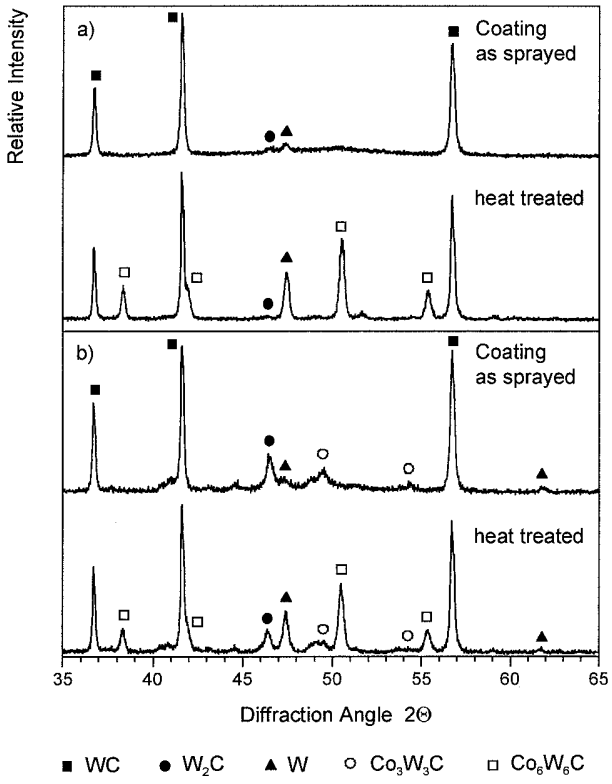

Fig. 5 Phase transformations of WC-Co coatings sprayed with DJ 2700 after 1 h heat treatment at 800 °C. (a) WC-Co 83-17 agglomerated sintered. (b) WC-Co 88-12 fused

sten, which can only be detected by x-ray analysis. Carbon seems to evaporate by oxidation as indicated by the lower carbon content of the coating compared to the powder. At the same time, part of WC dissolves in the cobalt matrix and can either form an amorphous or nanocrystalline supersaturated solid cobalt (tungsten, carbide) solution or an η-phase upon solidification. Tungsten and WC can precipitate from the supersaturated solid solution. In the scanning electron micrographs taken in the back scattered electron (BSE) mode, different gray shades of the matrix correspond to different amounts of tungsten and carbon dissolved in the cobalt and to different types of η-phases. Figure 4 shows the extent of phase transformations and amorphous solidification that can occur in the coatings.

When these coatings are heat treated at temperatures between 600 and 800 °C, the amorphous phase crystallizes to Co_6W_6C. Simultaneously, Co_3W_3C already present in the coating transforms to Co_6W_6C, and WC and tungsten are precipitated from the supersaturated solid solution within the matrix, indicated by the x-ray diffractograms of Fig. 5. The reactions lead to an increase of coating hardness, as shown in Fig. 6. The increase in hardness is related to the primary amount of amorphous phase in the coating.

3.4 Properties of the Coatings

The bond strength of all coatings was higher than 70 MPa and mostly exceeded the strength of the adhesive of 90 MPa. The hardness of the coatings sprayed with the agglomerated and sintered powder WC-Co 83-17 was between 980 and 1490 VHN, depending on the spray system used (Table 1). Coatings sprayed with the JP-5000, Top Gun-K, or the DJ 2600 and 2700 systems exhibited a higher hardness (1330 to 1490 VHN) compared to coatings sprayed with Jet Kote, Top Gun, and DJ Standard. The same trend was revealed by the bond strength, which was on average approximately 10 to 20 MPa higher. This can be related to the higher impact velocity of the particles, which is reached by these systems and results in a higher cohesive strength of the individual splats.

Carbon loss in the spray process ranging from 30 to 60% does not impair the hardness and wear resistance of the coatings (Fig. 7). Decarburization decreases the volume fraction of the carbides, but its detrimental effect on the hardness and wear resistance is compensated by the hardening of the cobalt matrix due to the solution of tungsten and carbide and the formation of hard and wear resistant W_2C and η-phases. Only when the carbon loss exceeds 60% are hardness and wear resistance reduced. Also at a carbon loss of less than 30% the hardness and wear resistance of the coatings are slightly lower. In this case the low carbon loss may indicate an insufficient heating of the particles.

Coatings from the different powders sprayed with the DJ 2700 system exhibited similar hardness and wear resistance, as shown in Table 2. The lower wear resistance of the WC-Co-Cr 86-10-4 coating can be explained by the high amount of Co_3W_3C being retained from the initial powder.

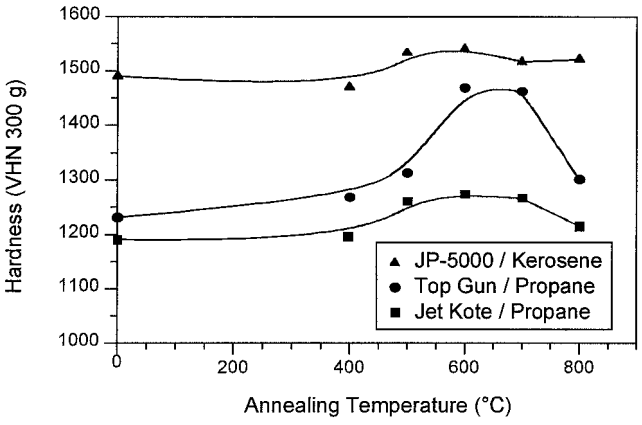

Fig. 6 Increase in hardness of WC-Co coatings after 1 h heat treatment at different temperatures

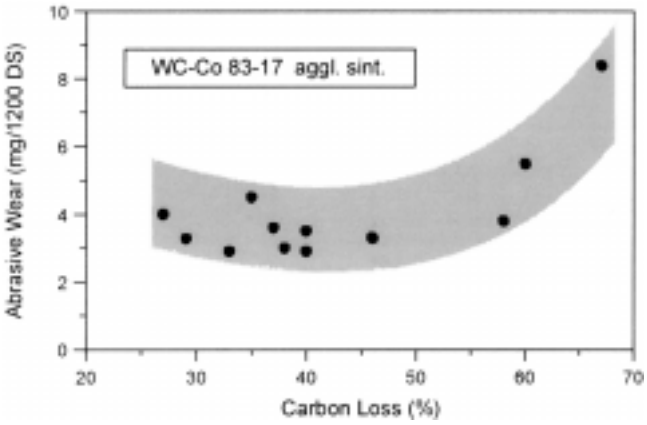

Fig. 7 Effect of carbon loss in the spray process on the wear resistance of WC-Co coatings

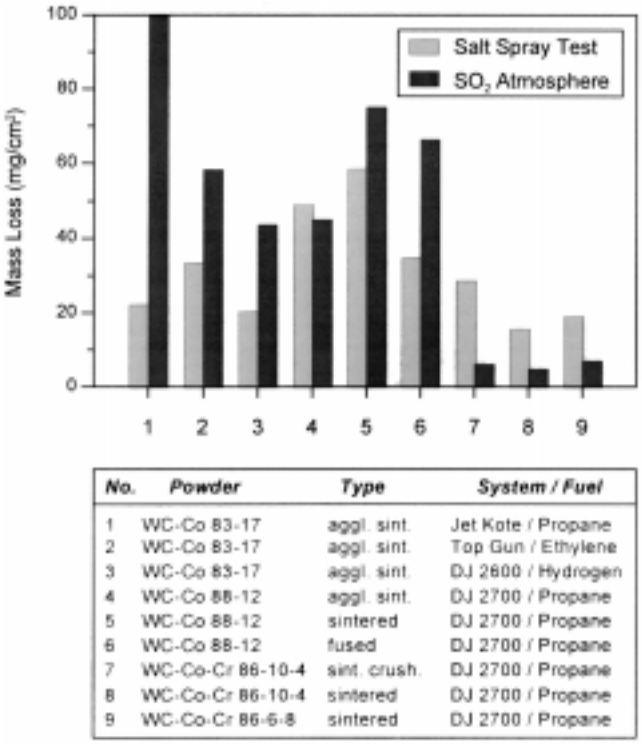

No.	Powder	Type	System / Fuel
1	WC-Co 83-17	aggl. sint.	Jet Kote / Propane
2	WC-Co 83-17	aggl. sint.	Top Gun / Ethylene
3	WC-Co 83-17	aggl. sint.	DJ 2600 / Hydrogen
4	WC-Co 88-12	aggl. sint.	DJ 2700 / Propane
5	WC-Co 88-12	sintered	DJ 2700 / Propane
6	WC-Co 88-12	fused	DJ 2700 / Propane
7	WC-Co-Cr 86-10-4	sint. crush.	DJ 2700 / Propane
8	WC-Co-Cr 86-10-4	sintered	DJ 2700 / Propane
9	WC-Co-Cr 86-6-8	sintered	DJ 2700 / Propane

Fig. 8 Mass loss of different WC-based coatings after corrosion testing in NaCl and SO_2 atmosphere

All coatings showed a rather high corrosion resistance. Mass loss after a 1200 h salt spray test and 50 cycles (50 days) in SO_2 atmosphere ranged from 5 to 100 mg/cm^2, which corresponded to a reduction in coating thickness from about 4 to 80 μm. Figure 8 demonstrates that the corrosion resistance of WC-Co-Cr coatings in general exceeds the resistance of WC-Co coatings, especially in SO_2 atmosphere. Metallographic investigation of corroded specimens showed a uniform corrosion attack of the surface, and none of the coatings exhibited corrosion down to the substrate. Only some coatings, which are not mentioned in the diagram of Fig. 8, failed during the tests by corrosion of the substrate at the interface, probably due to the higher porosity of those coatings.

4. Conclusions

During HVOF spraying of WC-based powders different kinds of phase transformations occur that determine the microstructure and chemistry of the coatings. The decarburization by oxidation of WC leads to the formation of W_2C and tungsten in the coatings, while the reaction of WC with the cobalt or cobalt-chromium matrix leads to a solution of tungsten and carbide in the matrix and can cause the formation of mixed carbides (η-phases). Moreover, the rapid solidification of the supersaturated cobalt (tungsten, carbon) matrix at impact of the particles results in the formation of an amorphous or nanocrystalline phase. The amount of amorphous phase in the coating is, therefore, determined by the amount of material that melts during the spray process.

The degree of phase transformations depends on the heat transferred to the particles in the respective spray system, on the flame temperature of the fuel used, and on the type of spray powder. Phase transformations increase when the injection of the powder occurs in a region where the flame temperature is highest such as for the Top Gun system, where the powder is injected directly into the combustion chamber. Less phase transformations occur when the powder is injected behind the combustion chamber in a region where the flame temperature is low, as in the JP-5000 and Top Gun-K system, or when the flame temperature is lowered by cooling air as in the DJ 2600 and 2700 systems. Also, the use of dense spray powders, which are heated up less in the spray process, or powders that already contain some amounts of η-phase reduce phase transformations.

Decarburization of an agglomerated and sintered WC-Co 83-17 powder ranges from 25 to 70% for the various spray systems and fuels. But the properties of the coatings such as hardness and wear resistance are not influenced when the carbon loss remains below 60%. Although the decarburization reduces the volume fraction of the carbides in the coatings, the surrounding matrix is hardened by the formation of a solid solution of cobalt (tungsten, carbon) and by the formation of hard and wear resistant W_2C and η-phases.

Hardness and bond strength of the coatings are mainly determined by the impact velocity of the particles, and are, therefore, higher when systems with a converging-diverging Laval nozzle are used, which provide superior particle velocities (Ref 20). However, the porosity of the coatings is also affected by the melting behavior of the particles. Dense powders, produced by sintering or fusing, are difficult to melt in the HVOF process. Thus, coatings sprayed with these powders show higher porosity, especially when spray systems are used that provide rather low heating of the particles. In respect to hardness, wear resistance and microstructure coatings of WC-Co-Cr are comparable to WC-Co coatings, however the corrosion resistance of WC-Co-Cr is considerably higher.

Acknowledgments

The spraying experiments were carried out in the laboratories of Linde AG, Höllriegelskreuth, Germany; GTV mbH, Luckenbach, Germany; and Tafa Inc., Concord, NH. The authors would like to thank them for providing equipment and technical support.

References

1. W.J. Jarosinski, M.F. Gruninger, and C.H. Londry, Characterization of Tungsten Carbide Cobalt Powders and HVOF Coatings, *Thermal Spray Coatings: Research, Design and Applications*, C.C. Berndt and T.F. Bernecki, Ed., ASM International, 1993, p 153-157
2. J.R. Fincke, W.D. Swank, and D.C. Haggard, Comparison of the Characteristics of HVOF and Plasma Thermal Spray, *Thermal Spray Industrial Applications*, C.C. Berndt and S. Sampath, Ed., ASM International, 1994, p 325-330
3. A. Karimi and C. Verdon, Hydroabrasive Wear Behaviour of High Velocity Oxyfuel Thermally Sprayed WC-M Coatings, *Surf. Coat. Technol.*, Vol 62, 1993, p 493-498
4. L.-M. Berger, P. Vuoristo, T. Mäntylä, W. Kunert, W. Lengauer, and P. Ettmayer, Microstructure and Properties of WC-Co-Cr Coatings, *Thermal Spray: Practical Solutions for Engineering Problems*, C.C. Berndt, Ed., ASM International, 1996, p 97-106
5. C. Verdon, A. Karimi, and J.L. Martin, Microstructural and Analytical Study of Thermally Sprayed WC-Co Coatings in Connection with their Wear Resistance, *Mater. Sci. Eng. A*, Vol 234-236, 1997, p 731-734
6. W. Coulson and S.J. Harris, The Microstructure of WC-Co Coatings Produced by HVOF Spraying with Liquid Fuel, *Trans. Inst. Met. Finish.*, Vol 73 (No. 3), 1997, p 108-112
7. A. Karimi, C. Verdon, and G. Barbezat, Microstructure and Hydroabrasive Wear Behaviour of High Velocity Oxy-Fuel Thermally Sprayed WC-Co(Cr) Coatings, *Surf. Coat. Technol.*, Vol 57, 1993, p 81-89
8. J. Nerz, B. Kushner, and A. Rotolico, Microstructural Evaluation of Tungsten Carbide-Cobalt Coatings, *J. Therm. Spray Technol.*, Vol 1 (No. 2), 1992, p 147-152
9. C.J. Li, A. Ohmori, and Y. Harada, Formation of an Amorphous Phase in Thermally Sprayed WC-Co, *J. Therm. Spray Technol.*, Vol 5 (No. 1), 1996, p 69-73
10. V. Ramnath and N. Jayaraman, Characterisation and Wear Performance of Plasma Sprayed WC-Co Coatings, *Mater. Sci. Technol.*, Vol 5, 1989, p 382-388
11. A. Karimi, C. Verdon, J.L. Martin, and R.K. Schmid, Slurry Behaviour of Thermally Sprayed WC-M Coatings, *Wear*, Vol 186-187, 1995, p 480-486
12. S.Y. Hwang, B.G. Seong, and M.C. Kim, Characterization of WC-Co Coatings Using HP/HVOF Process, *Thermal Spray: Practical Solutions for Engineering Problems*, C.C. Berndt, Ed., ASM International, 1996, p 107-112
13. C.J. Li, A. Ohmori, and Y. Harada, Effect of Powder Structure on the Structure of Thermally Sprayed WC-Co Coatings, *J. Mater. Sci.*, Vol 31, 1996, p 785-794
14. M.S.A. Khan, T.W. Clyne, and A.J. Sturgeon, Microstructure and Abrasion Resistance of WC-Co Coatings Produced by High Velocity Oxy-Fuel Spraying, *Thermal Spray: A United Forum for Scientific and*

Technological Advances, C.C. Berndt, Ed., ASM International, 1997, p 681-690
15. S. Usmani, S. Sampath, D.L. Houck, and D. Lee, Effect of Carbide Grain Size on the Sliding and Abrasive Wear Behavior of Thermally Sprayed WC-Co Coatings, *Tribol. Trans.*, Vol 40 (No. 3), p 470-478
16. EN 582, Thermal Spraying: Determination of Tensile Adhesive Strength, European Committee for Standardisation, 1993
17. JIS H 8615, Electroplated Coatings of Chromium for Engineering Purposes, Japanese Standards Association, 1995
18. DIN 50018, Prüfung im Kondenswasser-Wechselklima mit Schwefeldioxidhaltiger Atmosphäre, Deutsches Institut für Normung, 1997 (in German)
19. DIN 50021, Sprühnebelprüfungen mit Verschiedenen Natriumchlorid-Lösungen, Deutsches Institut für Normung, 1988 (in German)
20. H. Kreye, R. Schwetzke, and S. Zimmermann, High Velocity Oxy-Fuel Flame Spraying—Process and Coating Characteristics, *Thermal Spray: Practical Solutions for Engineering Problems*, C.C. Berndt, Ed., ASM International, 1996, p 451-456